Research paper

A systematic approach to the formulation of anti-onychomycotic nail patches

K. Rizi[a], I.K. Mohammed[b], K. Xu[a], A.J. Kinloch[b], M.N. Charalambides[b], S. Murdan[a],*

[a] Department of Pharmaceutics, UCL School of Pharmacy, 29-39 Brunswick Square, London WC1N 1AX, UK
[b] Department of Mechanical Engineering, Imperial College London, London SW7 2AZ, UK

ABSTRACT

Nail patches have a potential role as drug carriers for the topical treatment of nail diseases such as onycho-mycosis, a common condition. Our aim was therefore to develop a systematic and novel approach to the for-mulation of a simple drug-in-adhesive ungual patch. Twelve pressure-sensitive adhesives (PSAs), four backing membranes, two release liners and three drugs were screened for pharmaceutical and mechanical properties. From this initial screening, two PSAs, two drugs, one backing membrane and one release liner were selected for further investigation. Patches were prepared by solvent-casting and characterised. The patches had good uni-formity of thickness and of drug content, and showed minimal drug crystallisation during six months of storage. Meanwhile, the drug stability in the patch upon storage and patch adhesion to the nail was influenced by the nature of the drug, the PSA and the backing membrane. The reported methodology paves the way for a sys-tematic formulation of ungual nail patches to add to the armamentarium of nail medicines. Further, from this work, the best patch formulation has been identified.

1. Introduction

Onychomycosis, the fungal infection of the nail unit, affects 14–18% of the general population worldwide [1], and has been called a 'stub-born clinical problem' [2]. Its increasing incidence, significant negative impact on sufferers' quality of life [3] and current treatment limitations such as liver toxicity of oral drugs and low cure rates of approved to-pical medicines [4], demand new therapeutic approaches. Accordingly, we have studied the development of anti-onychomycotic nail patches. Topical therapy is highly desirable for its avoidance of systemic adverse effects and drug interactions. Therefore, a range of formulations such as lacquers, films, solutions, hydrogels and UV-curable gels have been investigated, as compiled in, for example [5,6]. Nail patches have also been investigated although the literature is very limited. It includes investigations into the influence of patch components on ungual (i.e. of the nail) drug permeation [7,8], testing of sertaconazole-containing patches in human volunteers[9], and the use of patches in photo-dynamic therapy of onychomycosis [10] and in iontophoretic ungual drug delivery[11].

An ideal nail patch should be easy to apply, remain adhered to the nail plate for the intended duration, release the loaded drug which can then permeate into the nail, be easy to remove cleanly when desired and be aesthetically acceptable. The design of a patch is obviously

critical to its performance. Our *aim* was, for the first time, to develop a systematic approach to the formulation of anti-onychomycotic nail patches, using a range of pharmaceutical and engineering tools. We present, in this paper, how these were used to examine and understand the related material, mechanical, rheological and pharmaceutical properties of the components and of the prepared patches, in order to optimise patch development.

The outline of the study is as follows. Firstly, the patch-type was selected. While various patch types are possible (as exemplified by commercially available skin patches [12–15]), we chose the drug-in-adhesive matrix type, where a drug-in-adhesive layer is sandwiched between a backing layer and a release liner for its simplicity. Secondly, the drugs terbinafine HCl, amorolfine HCl, and ciclopirox olamine, were selected as the model drugs, since terbinafine HCl is considered the oral anti-onychomycotic drug of choice in the UK [16], whilst the topical nail lacquers of amorolfine HCl and ciclopirox olamine have been the most effective topical preparations for many years, prior to the FDA-approval of Kerydin® and Jublia® in 2014. Thirdly, the other patch components, namely the adhesive, backing membrane and release liner were selected. The release liner and the backing layer must be chemi-cally inert, while the backing layer must also be aesthetically accep-table and flexible [15]. In addition, we decided to use a water-im-permeable backing layer in order to produce occlusive patches.

Occlusivity is expected to increase nailplate hydration, which is known to favour ungual drug permeation [17]. Enhanced nailplate hydration is also expected to convert drug-resistant fungal spores into drug-susceptible fungal hyphae, and this is expected to further enhance the success of topical anti-fungal therapy.

The adhesive is usually a pressure-sensitive adhesive (PSA), which is defined as a material which adheres to a substrate with light pressure and, ideally, leaves no residual adhesive upon its removal. It is one of the most critical components of the patch [13,18]. The PSA must adhere to the substrate, be biocompatible as well as compatible with the drug and excipients, remain stable and functional once formulated in the patch, provide adequate diffusivity to the drug, and be acceptable to the regulatory authorities [13]. Commonly used PSAs in skin patches include polyisobutylenes (PIBs), polysiloxanes (silicones) and polyacrylate copolymers (acrylics) [13–15], and within each of these groups, there are many commercially-available options. In this work, the Hansen Solubility Parameter (HSP) concept was used in order to select the optimum PSAs which would enable a high drug loading, which was desired as it could be expected to lead to a large drug reservoir in the patch, reduced frequency of patch application and thereby enhanced patient adherence.

Following selection of the patch components, drug-loaded patches were prepared, and the preparation method was optimised. Prepared patches were characterised to enable the optimisation of the formulation of novel anti-onychomycotic nail patches.

2. Materials and methods

2.1. Materials

Amorolfine HCl (Ranbaxy Research Laboratories, India), terbinafine HCl (AK Scientific, USA) and ciclopirox olamine (Zhejiang Huadee Chemicals, China) were used as model antifungal drugs. Pressure Sensitive Adhesives (PSAs) were supplied as solutions of the polymer in organic solvents, and the solid content of the solutions was gravimetrically measured. Duro-Tak™ acrylic adhesives (grades: 87-4098, 87-9301, 87-2852, 87-504A, 87-202A, 87-4287, 87-502A and 87-2525) were kindly provided by Henkel Ltd, UK. Silicone adhesives, Bio-PSA 4102, Bio-PSA 4202 and Bio-PSA 4302, were obtained from Dow Corning, USA. Oppanol B15 polyisobutylene adhesive was not used experimentally, but its HSP values were obtained from the HSPiP software. Four different backing membranes (Scotchpak 9723, Scotchpak 9733, Scotchpak 9757 and CoTran 9701 were purchased from 3M, UK. The 3M Scotchpak 9744 (a polyester film with a fluoropolymer release-coating applied to one side) was selected as the release liner following initial experiments with two potential liners (i.e. Scotchpak 1022 and Scotchpak 9744) and the determination of a lack of significant difference between the two. For the peel tests, three different materials were used as substrates: high density polyethylene (HDPE, 4 mm thick, (RS, Corby, UK), Vitro-Nail® (a commercially-available polymeric material marketed as a possible model for the human nail plate, IMS Inc., Portland, USA) and human cadaver nails (Tissue Solutions, UK).

Trifluric acid (TFA), phosphoric acid, triethylamine, acetonitrile, sodium octane sulfonate and methanol were purchased from Sigma-Aldrich (UK) and were of HPLC grade. Solvents used to determine the values of the HSP of the PSAs included 1,3-dioxolane, 1-butanol, 1-methyl-2-pyrrolidone, 1-pentanol, 2-(methylamino)ethanol, 2,2,4-trimethylpentane, 4-hydroxy-4-methyl-2-pentanone (diacetone alcohol), acetic acid, acetic anhydride, acetophenone, benzyl alcohol, benzyl butyl phthalate, butyl acetate, chlorobenzene, chloroform, dibutyl phthalate, diethylene glycol, DMSO, dodecanol, ethanol, ethanolamine, ethylene glycol monomethyl ether, isopropyl palmitate, methyl ethyl ketone, dichloromethane, N,N-dimethylformamide, octanol, phosphoric acid, propane, propylene carbonate, p-xylene, tetrahydrofuran, toluene, trimethylamine, vinyl pyrrolidone were

obtained from Sigma Aldrich (UK), acetone, acetonitrile, benzaldehyde, formaldehyde, methanol (Fisher Scientific, UK) and heptane (BDH Chemicals Ltd, UK).

2.2. Selection of appropriate pressure sensitive adhesives for high drug loading

Hansen Solubility Parameters (HSPs) were used to select the appropriate PSAs. HSPs divide the total solubility parameter, δ_T, into individual parts arising from dispersion forces, δ_D, permanent dipole-permanent dipole forces, δ_P, and hydrogen bonding forces, δ_H, [19] as follows:

$$\delta^2{}_T = \delta_D^2 + \delta_P^2 + \delta_H^2 \tag{1}$$

To determine the compatibility between a PSA and a drug, the solubility parameter 'distance' between them (R_a) was calculated from their respective HSPs as follows:

$$(R_a)^2 = 4(\delta_{D2}-\delta_{D1})^2 + (\delta_{P2}-\delta_{P1})^2 + (\delta_{H2}-\delta_{H1})^2 \tag{2}$$

where the subscripts 1 and 2 refer to PSA and drug, respectively.

A smaller R_a indicates higher PSA-drug compatibility, which is expected to lead to higher drug loading in the patch. Thus, to identify appropriate PSAs for each anti-fungal drug, the HSPs of the drug and of the PSAs were determined, and PSA-drug R_a values were calculated.

2.2.1. Determination of the HSPs of the pressure sensitive adhesives and of the drugs

HSPs of the Duro-Tak™ acrylic adhesives (grades: 87–4098, 87-9301, 87-2852, 87-504A, 87-202A, 87-4287, 87-502A and 87-2525) and of the silicone adhesives (Bio-PSA 4102, Bio-PSA 4202 and Bio-PSA 4302) were experimentally determined while the HSP of the polyisobutylene PSA (Oppanol B15) was taken from the Hansen Solubility Parameters in Practice (HSPiP) software (3rd edition 3.1.12, Steven Abbott TCNF Ltd, UK). For the experimental determination of the values of the HSPs, small amounts of a PSA or drug were weighed into vials and a solvent was added to each vial to give a PSA concentration of 100 mg/ml or a drug concentration of 10 mg/ml. The mixtures were stirred at 25 ± 1 °C for 72 h to allow time for complete dissolution, if this was achievable. The vials were then visually inspected, and the solvents were scored as: good (i.e. 1) if the PSA had completely dissolved in the solvent and bad (i.e. 0), if not. Experiments were conducted in triplicate. The solvent scores were then inputted into the HSPiP software. This software plots the δ_D, δ_P and δ_H of each organic liquid along the axes of a 3-dimensional graph, and locates a sphere in the HSP space that includes all or most of the 'good' solvents and excludes the 'bad' ones, with a minimum of error, as indicated by the 'fit'. The central coordinates of the sphere give the values of the HSPs (i.e. δ_D, δ_P, δ_H) of the PSA. Multiple calculations allowed the calculation of the mean values and standard deviations. For each PSA, between forty and fifty liquids were tested, and the number of good solvents ranged from fifteen to thirty four for the different PSAs. For each drug, between thirty three and thirty nine liquids were tested. The HSPs of the drugs have been reported previously [20]. For both drugs and PSAs, fits of greater than 0.9 were obtained.

2.2.2. Theoretical and experimental determination of drug-PSA affinities

Once the HSPs of the drugs and PSAs had been determined (Section 2.2.1, their theoretical compatibility (indicated by R_a) was calculated using Eq. (2). The experimental drug-PSA affinity was measured by examining drug-in-PSA films by polarised light microscopy. Solutions of drug in PSA (with drug loadings of 0 to 20% w/w) were prepared, cast over a defined area onto microscope slides, left to dry for 72 h at room temperature, and the resulting films were examined under a Nikon Microphot-FXA microscope (Tokyo, Japan) for the presence of drug crystals. Micrographs where taken with a Lumenera Infinity-2 digital camera (Ottawa, Canada) and analysed with ImageJ software (Version

1.45s, from the National Institutes of Health, Bethesda, Maryland, USA) for the percentage area covered in drug crystals.

2.3. Measurement of the mechanical and rheological properties of the PSAs

2.3.1. Casting of the PSAs

The HSPs-based work described above identified Duro-Tak 87-2852 and Duro-Tak 87-202A (henceforth referred to as Duro-Tak 2852 and Duro-Tak 202A, respectively) as the optimal PSAs to give the highest drug loadings. The mechanical and rheological properties of these two PSAs were therefore characterised. All experiments were performed at 21 °C and 50% humidity, using a Zwick Roell 1.0 mechanical testing machine (Zwick Testing Machines Ltd., UK) equipped with a 1 kN load cell. The PSA films were prepared by diluting the PSAs with dichloromethane (DCM) at a weight ratio of 2:3, casting the solution onto a release liner (200 mm × 150 mm) which was placed in a mould, allowing the solvent to evaporate for at least 24 h at room temperature, followed by the placement of a second sheet of release liner on the PSA surface, thereby creating a liner-PSA-liner sandwich. To prepare drug-loaded PSA films, the drug was dissolved in the PSA-solvent mixture and the solution was left to stand for 24 h prior to casting.

2.3.2. Determination of the tensile properties of the PSA films

Liner-PSA-liner sandwich films, prepared as described above, were cut into 90 mm by 10 mm samples. One release liner was removed and the resulting PSA-liner was stuck to the inner surface of the tensile grips, set 50 mm apart. Thus, the value of the tensile gauge length, L, was 50 mm. The second release liner was removed and the PSA film was clamped between the tensile grips. Tensile tests on drug-free and drug-loaded PSA films were performed at constant speeds of 1, 10 and 100 mm/min, giving true strain rates of 0.1, 1 and 10/min respectively. The true stress, σ, and true strain, ε, were calculated from the load, F, and displacement, δ, data using Eqs. (3) and (4) respectively:

$$\sigma = \frac{F}{bt}\left(1, + , \frac{\delta}{L}\right) \tag{3}$$

$$\varepsilon = ln\left(1, + , \frac{\delta}{L}\right) \tag{4}$$

where b is the sample width and t is the sample thickness (which was in the range of 600–800 μm).

2.3.3. Determination of the tack of the PSAs

PSA samples (approximate thickness 200 μm) were prepared by diluting the PSAs, as described above, casting the solutions onto a high-density polyethylene (HDPE) surface, and allowing the solvent to evaporate for 24 h. A flat steel probe of diameter 6 mm was lowered onto the PSA sample, allowed to dwell for 60 s at dwell forces of 0.5 N, 4.5 N or 10 N and then pulled off at a speed of 10 mm/min. The resulting load-displacement data was converted into stress-displacement curves to obtain the tack strength, σ_{max}, and the tack work of adhesion, W_a, which was calculated as the area under the curve.

2.3.4. Measurement of surface energies of PSAs and of model nail plates

The surface energies of the Duro-Tak 2852 and Duro-Tak 202A PSAs and of the model nail plates were measured: (a) as an indicator of the patch adhesion to the nail plate, since the adhesion is known to depend on the surface energies of the surfaces involved [14], and (b) to correlate later with the peel tests results. Due to the cost, scarcity and natural curvature of human nail plates in both directions [21], which make peel tests challenging, peel tests were also conducted using two other model substrates, namely, Vitro-Nail® (claimed to mimic the wetting properties of human fingernails [22] and HDPE, which has previously been found to be a suitable model for the nail plate in adhesion experiments [23,24]. Model nail plates should have similar surface energies to that of the human nail plate, given that adhesion is

related to the surface energies of the surfaces involved.

The surface energies of the PSAs and the model nail plates were determined via the measurement of contact angles formed by droplets of four liquids (i.e. water, glycerol, diiodomethane and formamide) on the sample surface using a goniometer. A droplet of a liquid was placed onto the sample surface using a syringe, imaged using the goniometer camera and the contact angle was determined. For each liquid, ten images were taken at two second intervals and the contact angle on both sides of the droplet of each image was measured. The average of twenty measurements was taken, and used to calculate the sample's surface energy using the Kinloch, Kodokian Watts (KKW) method [25]. Once the surface energies of the PSAs and model nail plates were determined, the thermodynamic work of adhesion, ψ_a, between the PSA and the model nail plate was calculated using:

$$\psi_a = 2\sqrt{\gamma_{S_1}^d \gamma_{S_2}^d} + 2\sqrt{\gamma_{S_1}^p \gamma_{S_2}^p} \tag{5}$$

Where γ_s^d and γ_s^p are, respectively, the dispersion force and the polar force components to the total surface free energy (γ_S) of a solid, where $\gamma_S = \gamma_s^d + \gamma_s^p$ and the numbers 1 and 2 relate to the two materials (i.e. the PSA and model nail plate).

2.4. Selection of the optimal backing membranes

2.4.1. Determination of the occlusivity of backing membranes

The occlusivity of the backing membranes Scotchpak 9723, 9733, 9757 and CoTran 9701 were assessed by measuring their moisture vapour transport, as per ISO 2528 (1995) International Standard. Beakers containing water and enclosed with a backing membrane were placed in a water-bath at 32 °C (to mimic the body surface temperature) and weighed at time intervals to measure the water loss from the beaker.

2.4.2. Determination of the tensile properties of backing membranes

A backing membrane which was stiff enough, so that it would not deform considerably, and which was strong enough, to prevent patch breakage upon the latter's removal from the nail, was required. The tensile properties of the four backing membranes were therefore assessed at speeds of 10, 100 and 1000 mm/min using a 1 kN load cell and backing membrane samples of 130 mm × 10 mm. The load-displacement data was converted to a stress-strain plot, using Eqs. (3) and (4), and the Young's modulus, E, and yield stress, σ_y, were obtained.

2.4.3. Determination of backing membrane behaviour in peel tests

Peel tests, using a range of backing-membrane/PSA combinations, adhered to the HDPE model nail plate, were conducted to identify the optimal backing-membrane/PSA combination, using the set-up as shown in Fig. 1. Patches were prepared as described in Section 2.5 below, then cut into strips (20 mm × 80 mm). The release liner was removed and approximately 40 mm of the patch strip was stuck to the HDPE, by rolling a 1 kg weight roller once over the patch, while the other end of the patch strip was fixed to a tensile grip on the mechanical testing machine. The HDPE itself was attached to a 80 mm × 40 mm precision linear slide with a stroke length of 47 mm, which ensured the maintenance of a constant peel angle during the test. Peel tests were conducted at peel speeds of 1, 10 and 100 mm/min and at a peel angle of 90°.

2.5. Preparation of drug-loaded nail patches

Nail patches were prepared by diluting the purchased PSA solution with DCM to obtain a PSA concentration of 15% w/w. Different amounts of drugs were added to the polymer solutions to obtain drug loadings at the dissolved saturation level in each polymer. The mixtures were then cast onto the selected backing membrane contained in moulds (7.5 cm × 5 cm) and the solvent was allowed to evaporate for
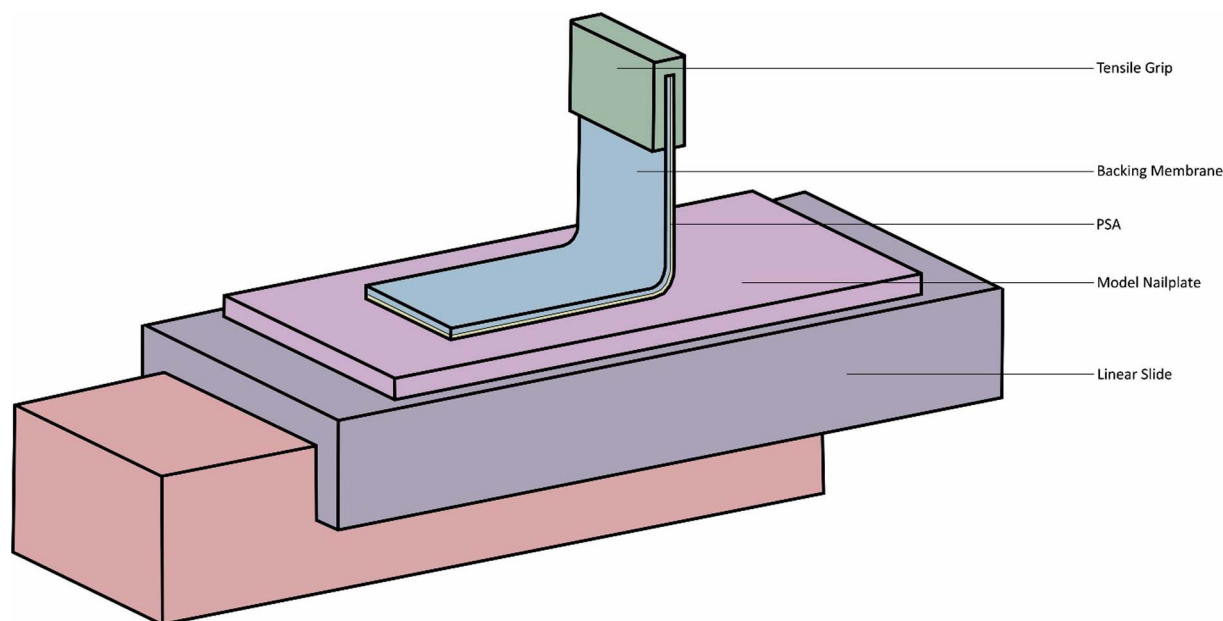
Fig. 1. A schematic of the experimental peel test at 90°.

24 h. Subsequently, the release liner was placed on the PSA surface to create a backing membrane-PSA-liner sandwich.

2.6. Characterisation of the drug-loaded nail patches for thickness, residual solvent, and drug load uniformity, homogeneity and stability

Thickness of the prepared patches was measured at ten different positions using a digital micrometer.

Residual solvent in the patch was measured by thermogravimetric analysis using a Discovery TGA instrument (TA instruments Ltd, UK). The patches were heated to 80 °C, due to drug instability above 100 °C, then maintained at 80 °C for one hour until the weight loss remained constant.

Uniformity of drug content was measured by cutting patches into 1 cm^2 sections, which were then weighed and dissolved in 20 ml of methanol. These samples were stirred overnight, sonicated for 30 min, filtered (with a PTFE syringe filter with a pore size of 0.45 μm) and the drug content was determined using HPLC (as described below), following appropriate dilution with a 40:60 acetonitrile: water mixture.

Homogeneity of the drug loading in the patch was analysed by Raman spectroscopy and X-ray photoelectron spectroscopy (XPS). Raman spectra of patches, drug-free PSAs and pure drugs were obtained using the Renishaw inVia micro-Raman system equipped with a 300 mW near-infrared diode laser at a wavelength of 785 nm for excitation (Renishaw Inc., UK) using a 20x objective lens. Spectra were recorded with a resolution of 1 cm^{-1} in the range of 400–3500 cm^{-1} and obtained for a 10 s exposure of the CCD detector. To establish the drug distribution within the PSA, depth profiling of the patches was performed by scanning their cross sections at eight different points at intervals of 40 μm.

XPS was conducted on both surfaces of a drug-loaded PSA layer, as well as on a cross-section to determine the drug distribution in the patch. The nitrogen, oxygen and carbon compositions were measured, with the nitrogen (which is present in the drug, but not in the PSA) giving evidence of drug presence. To analyse the interior of a patch, the patch was etched at nine levels for 10 s each time. The XPS instrument (Thermo K-alpha spectrometer, UK) utilised a 72 W monochromated Al Kα X-ray source, focused to a spot of 400 μm diameter at the sample surface. The electron energy analyser operated in a constant analyser energy (CAE) mode with a 128 channel position sensitive detector. The pass energy was set to 151.2 eV. Spectra were analysed using the Thermo Avantage software.

To measure drug stability in the patches, the patches were stored for six months under accelerated (40 °C/75% RH) test conditions and drug levels were measured at monthly intervals by HPLC, as described below. In addition, the ciclopirox olamine-loaded patches were stored under long-term (25 °C/60% RH) test conditions, and were examined by microscopy at monthly intervals (as described in Section 2.2.2) to determine the presence and growth of any drug crystals.

HPLC was conducted using a 1260 Infinity Agilent HPLC system using a Luna C18 column (150 × 4.6 mm, 5 μm). For amorolfine HCl and terbinafine HCl, a flow rate of 1 ml/min and an injection volume of 20 μl were used with UV detection at 220 nm and 224 nm respectively. The mobile phase for amorolfine HCl consisted of 0.1% TFA in water and acetonitrile at a ratio of 55:45 v/v and resulted in the elution of the drug after 4.8 min. For terbinafine HCl, a mobile phase of 0.012 M trimethylamine and 0.020 M phosphoric acid was mixed with acetonitrile (65:35 v/v). The retention time for terbinafine was 6.1 min. For the drug ciclopirox olamine, a mobile phase of 5 mM sodium octane sulfonate in water and acetonitrile (50:50 v/v) was employed using a flow rate of 2 ml/min, a UV detection of 267 nm and an injection volume of 40 μl. This resulted in the elution of ciclopirox olamine at 3.1 min. The HPLC methods were validated for linearity, accuracy, precision (intra-day and inter-day) and limits of detection and quantification.

2.7. Peel tests on patches

Peel tests on drug-loaded patches (with PSA thickness of approximately 200 μm) were conducted using the two nail plate models (i.e. HDPE and Vitro-Nail) as well as a human cadaver nail plate, as described in Section 2.4.3, at constant peel speeds of 100 mm/min and a peel angle of 90°. The human cadaver nail plates were softened by placing them in a hot water bath for approximately ten minutes, then flattened (by placing a 5 kg weight on top of the nail plates overnight) and then bonded to a rigid aluminium plate using an epoxy adhesive, i.e. Araldite® Rapid, UK.

2.8. Statistical analysis

The IBM Statistical Package for the Social Sciences 22 software was used. In all cases, p ≤ 0.05 was used to assess the degree of statistical significance. Repeated-measures ANOVA tests were conducted to

Table 1
Hansen Solubility Parameters of PSAs considered for use in ungual patches. HSPs were experimentally determined except for Oppanol B15*, whose HSP values were taken from the Hansen Solubility Parameters in Practice (HSPiP) software. Means ± SD are shown.

PSA name	Description	Functional groups	δ_D	δ_P	δ_H
		Hansen Solubility Parameters (MPa$^{\frac{1}{2}}$)			
Duro-Tak 87-202A	Acrylic	–OH	17.2 ± 0.3	8.7 ± 0.5	6.5 ± 0.3
Duro-Tak 87-2852	Acrylic	–COOH	16.4 ± 0.2	5.6 ± 0.3	6.9 ± 0.2
Duro-Tak 87-9301	Acrylic	none	16.4 ± 0.1	5.5 ± 0.3	6.7 ± 0.3
Duro-Tak 87-4287	Acrylate- vinylacetate	–OH	16.6 ± 0.1	6.1 ± 0.1	6.1 ± 0.1
Duro-Tak 87-2525	Acrylate-vinylacetate	–OH	16.6 ± 0.1	6.3 ± 0.3	6.4 ± 0.1
Duro-Tak 87-4098	Acrylate-vinylacetate	none	16.6 ± 0.1	6.4 ± 0.1	6.6 ± 0.1
Duro-Tak 87-504A	Acrylic-rubber hybrid	–OH	15.8 ± 0.2	1.2 ± 0.4	5.4 ± 0.5
Duro-Tak 87-502A	Acrylic-rubber hybrid	–OH	15.7 ± 0.3	2.3 ± 0.2	4.8 ± 0.3
Bio-PSA 4102 Bio-PSA 4202 Bio-PSA 4302	Silicone	–Si(CH$_3$)$_3$	16.1 ± 0.1	1.9 ± 0.4	5.0 ± 0.2
Oppanol B15	Polyisobutylene	None	18.8*	1.5*	1.3*

determine whether there was any influence of drug loading on the tensile properties of the PSAs. A two-way between-groups ANOVA was conducted to explore the impact of dwell force and of the nature of the PSA on the tack strength, and on the tack work of adhesion. A two-way ANOVA was also conducted to explore the influence of the nature of the substrates, and of the drug, on the patch peel force.

3. Results and discussion

3.1. Selection and characterisation of the PSAs

3.1.1. Selection of PSAs for high drug loading

The Hansen Solubility Parameters of the PSAs are shown in Table 1. It can be seen that the experimentally-determined δ_D, δ_P and δ_H parameters reflected the chemical structures of the PSAs. Thus, the acrylic and acrylate-vinylacetate PSAs, with their hydroxyl and carboxyl groups, showed greater values of δ_P and δ_H compared to the acrylic-rubber hybrids, silicone- and polyisobutylene-based PSAs. The HSPs of the anti-onychomycotic drugs are shown in Table 2. As expected, these drug salts showed relatively high δ_P and δ_H values.

For each PSA-drug combination, the theoretical and experimental compatibilities are shown in Table 3, which shows a general trend of decreasing drug solubility in the PSA with increasing R_a (i.e. the solubility parameter 'distance' between drug and PSA). Thus, to some extent, the theoretical and actual compatibilities agree, although the trend is far from perfect, which shows that, while HSP values can be used to predict drug-PSA compatibility, the degree of compatibility must be experimentally confirmed. Table 3 also shows the presence of a notable outlier, Duro-Tak 2852 PSA, in which the drugs are far more soluble than in the other PSAs with similar R_a values. It seems that the

Table 2
Hansen Solubility Parameters of drugs considered for use in ungual patches, from [20]. The mean and (SD) values are shown. Molar volumes and log P are predicted values from Chemistry Dashboard https://comptox.epa.gov/dashboard).

Drug	Hansen Solubility Parameters (MPa½)			Other properties from https://comptox.epa.gov/dashboard)		
	δ_D	δ_P	δ_H	MW (Da)	Molar volume (cm^3)	Log Partition coefficient P
Amorolfine HCl	18.1 (0.4)	12.2 (0.5)	16.9 (0.3)	354	343	5.3
Terbinafine HCl	17.1 (0.7)	16.6 (1.1)	13.9 (0.6)	328	289	5.9
Ciclopirox olamine	17.4 (0.6)	13.9 (0.6)	17.2 (0.6)	268	174	2.1

carboxylic groups in this PSA enhance drug solubility, possibly due to interactions with the amine moieties in the drugs, whose chemical structures are shown in Supplementary file, 1. The greater solubility of the ciclopirox olamine compared to those of amorolfine HCl and terbinafine HCl, could be due to its smaller molecular size (shown in Table 2), as well as its more basic primary amine group, which could interact to a greater extent with the carboxylic groups of the Duro-Tak 2852 PSA. For all three drugs, the most promising PSAs are shown to be the acrylic adhesives, Duro-Tak 2852 and the Duro-Tak 202A, which enabled the greatest drug loadings.

The suitability of these two PSAs were therefore further examined. To investigate the influence of drug loading, if any, on the mechanical properties of the PSAs, amorolfine HCl and ciclopirox olamine were used at their saturation solubilities in each PSA, i.e. ciclopirox olamine at 5% in Duro-Tak 202A and at 16% in Duro-Tak 2852; and amorolfine HCl at 3% in Duro-Tak 202A and at 5% in Duro-Tak 2852. Amorolfine HCl and ciclopirox olamine were both included in order to assess the effects of the nature and concentration of the drug on the properties of the PSAs. Meanwhile, terbinafine HCl was excluded from further study, given the similarities in the solubility profiles of amorolfine HCl and terbinafine HCl in the different PSAs.

3.1.2. Mechanical properties of PSAs

Typical stress-strain curves of the two selected PSAs are shown in Fig. 2. A large difference is seen, with the Duro-Tak 2852 showing a higher modulus and a higher fracture stress. In addition, Duro-Tak 2852 fails in tension at a strain of approximately 2.1 (equivalent to the PSA film stretching approximately seven times its original length) whereas the Duro-Tak 202A has not yet failed at the maximum test strain reached (i.e. of 2.4, equivalent to the film stretching to ten times its original length). Thus, Duro-Tak 202A exhibits a greater strain to failure. This indicates that in practice, i.e. when a patient is peeling a patch off from their nail, the Duro-Tak 202A PSA would be more likely to stretch, making it more difficult and painful to remove. For both PSAs, an effect of test rate is shown, with a less stiff response at the lower rate as the viscoelastic PSA has more time to flow and elongate and therefore needs a smaller force to achieve a given level of strain.

To investigate the influence of drug loading, Duro-Tak 2852 PSA was selected due to its stiffer mechanical response (which would allow any changes to be more obvious), and the influences of amorolfine HCl and ciclopirox olamine addition are shown in Fig. 3. For both drugs, a less stiff stress-strain response was seen, compared to the drug-free control (p < 0.05), that is, the drugs plasticise the PSA. The plasticising effect of amorolfine HCl was very similar to that of ciclopirox olamine (repeated-measures ANOVA p > 0.05), despite its much lower concentration, i.e. 5% versus 16% (or 0.01 mol versus 0.06 mol per 100 g). This shows that the plasticisation effect was not due to the

Table 3

Theoretical and experimental determinations of PSA-drug compatibility. Theoretical determinations are shown by R_a, where the larger the R_a, the lower the compatibility. Experimental determinations are shown by the drug concentration (%w/w) loaded into a PSA at which drug crystals start to appear.

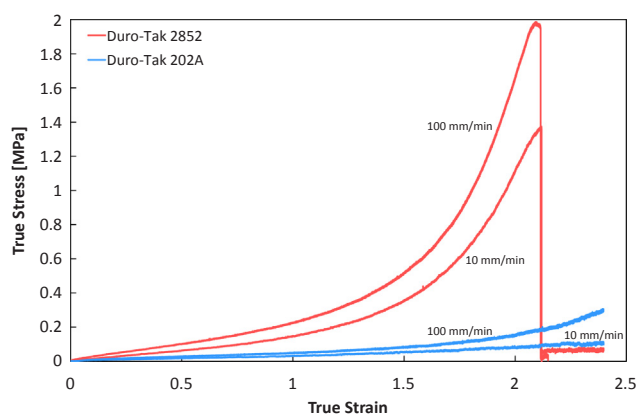| PSA name	Terbinafine HCl		Amorolfine HCl		Ciclopirox olamine	
	R_a	Drug concentration at which crystals start to appear (%)	R_a	Drug concentration at which crystals start to appear (%)	R_a	Drug concentration at which crystals start to appear (%)
Duro-Tak 202A	11	4	11	4	12	6
Duro-Tak 2852	13	8	12	7	13	17
Duro-Tak 9301	13	1	13	2	14	1
Duro-Tak 4287	13	2	13	1	14	3
Duro-Tak 2525	13	2	12	2	13	1
Duro-Tak 4098	13	1	12	1	13	1
Duro-Tak 504A	18	1	17	1	18	3
Duro-Tak 502A	17	1	16	1	17	3
Bio-PSA 4102	17	1	16	1	17	1
Bio-PSA 4202						
Bio-PSA 4302						
Oppanol B15	20	ND	19	ND	20	ND

Fig. 2. Typical tensile stress-strain curves of the drug-free PSAs: Duro-Tak 2852 (– red, top 2) and Duro-Tak 202A (– blue, bottom 2); at test speeds of 10 and 100 mm/min.
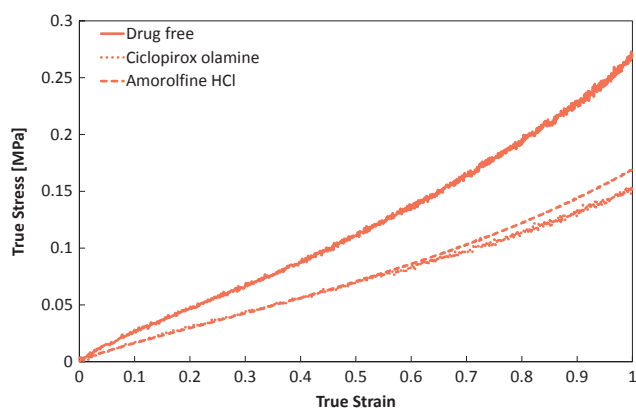

Fig. 3. Typical tensile stress-strain curves at a testing true strain rate of 1 min^{-1} for drug-free and drug-loaded Duro-Tak 2852 PSAs. The ciclopirox olamine drug was present at 16% w/w while the amorofine HCl drug was present at 5% w/w.

Fig. 4. Tack strength, σ_{max}, and tack work of adhesion, W_a, for the drug free Duro-Tak 2852 (•) and Duro-Tak 202A (x) PSAs adhering to the HDPE substrate. Means and SDs (error bars) are shown. N = 4–5.

amount of drug loaded in the PSA, but rather due to the chemical nature of the drugs which would govern any drug-PSA interactions. In practice, any reduction in the stiffness of the PSA by drug loading could lead to a greater difficulty being encountered during patch removal from a nail plate, as the PSA would stretch more and tend to fibrillate rather than peel off the nail.

3.1.3. Tack of the PSAs

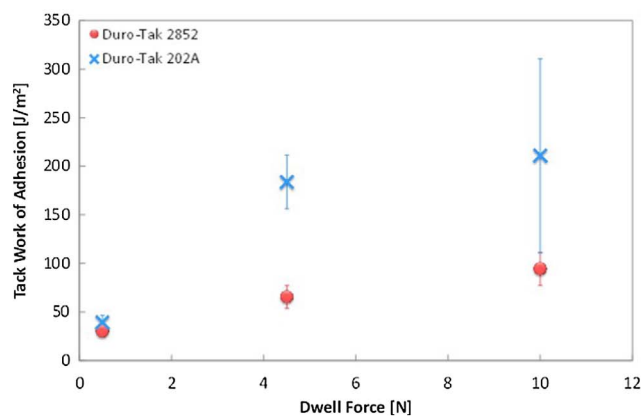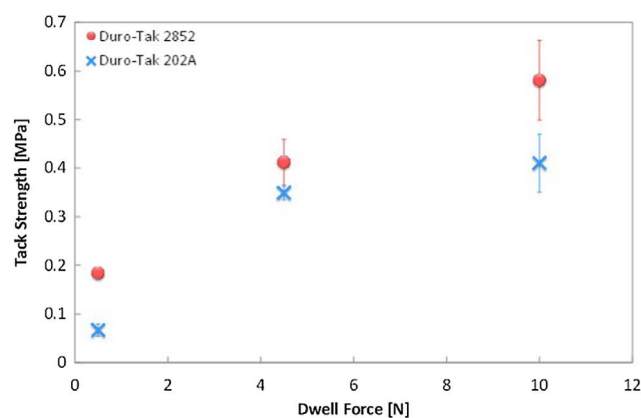The tack strength, σ_{max}, and the tack work of adhesion, W_a, of the two PSAs are shown in Fig. 4. As expected, increasing the dwell force increased the tack strength and the tack work of adhesion for both PSAs ($p < 0.05$). Duro-Tak 2852 showed a greater tack strength compared to the Duro-Tak 202A at all dwell forces ($p < 0.05$). From this observation, it was expected that Duro-Tak 2852 PSA would give a higher tack work of adhesion compared to Duro-Tak 202 PSA. Surprisingly, this was not so. The opposite was observed, which is related to the way the tack work of adhesion, W_a, was calculated, i.e. from the area under the stress-displacement curve. The value of W_a was higher for Duro-Tak 202A as its tensile failure occurred at a much greater displacement than for Duro-Tak 2852, in agreement with the tensile results shown in Section 3.1.2. These results indicate that, while a higher stress may be

needed to remove a patch based on Duro-Tak 2852 PSA from a nail plate, more energy will be needed to remove a patch containing Duro-Tak 202A, as the latter adhesive elongates to a greater extent while it is being peeled off from a nail plate. In practice, the higher W_a for Duro-Tak 202A might lead to more fibrillation (due to its ability to deform more easily) and potentially lead to undesired PSA residue remaining on the nail plate upon patch removal from a nail. Meanwhile, the higher tack strength of Duro-Tak 2852 would mean that it is less likely to fall off during normal wear, although the higher force needed to remove the patch when desired may mean a more painful patch removal.

3.1.4. Surface energies of the PSAs and of model nail plates and PSA-nail thermodynamic work of adhesion

The surface energies of the model nail plates and of the PSAs are shown in Table 4. It can be seen that the surface energies of the various PSAs are fairly similar in value, with the dispersion component making, by far, the greater contribution. The surface energies of the PSAs being approximately 30 mJ/m^2 is promising for their application in ungual patches, given that for good intrinsic adhesion, the surface energy of the adhesive must be equal to, or less than, that of the substrate[14], and that the surface energy of the human nailplate in vivo has been found to be 34.1 $\pm$ 5.5 mJ/m^2 [26]. The surface energy of 38 mJ/m^2 for HDPE is in good agreement with previously reported values of 35 mJ/m^2 [27] and 40 mJ/m^2 [23], and is close to the surface energy of a human nail plate [26]. Thus, HDPE appears to be a better model for the human nail plate than Vitro-Nail and is therefore used in the peel experiments reported below. The values of the thermodynamic work of adhesion, ψ_a, between the model nail plates and the PSAs are also shown in Table 4. It can be seen that ψ_a is somewhat higher for the PSAs adhering to the Vitro-Nail, which is due, of course, to its higher surface energy compared to HDPE. Otherwise, there is little difference in the values of ψ_a amongst the various PSAs.

Drug inclusion in the PSA has a minimal influence on the surface

energy of the PSAs and consequently on the thermodynamic work of adhesion, which is possibly due to (a) the relatively small amounts of drug in the PSAs, and (b) the fact that the drug was in a molecularly dispersed form, rather than a particulate form whose relatively large size could have changed the surface and interface properties.

It is worth commenting here that the thermodynamic work of adhesion, ψ_a, is orders of magnitude smaller that the tack work of adhesion, W_a, shown in Fig. 4. This was expected due to the highly viscous dissipative deformation of the PSA, which accompanies the interface rupturing, and so leads to $W_a >> \psi_a$.

3.2. Selection of the backing membrane

3.2.1. Colour, thickness and moisture vapour transmission rates

The polymeric nature, colour, thickness and moisture vapour transmission rates of the four backing membranes are shown in Table 5. All the backing membranes are relatively thin ($\leq$ 50 μm). The tan colour of Scotchpak 9723 is presumably due to the fact that it is supplied for the fabrication of skin patches [28] and the tan colour would provide a degree of camouflage when a patch is worn on the skin. For application to a nail patch, however, a translucent backing membrane would be more appropriate and provide a greater camouflage and patient acceptability. CoTran 9701 is much more permeable to water vapour than the other backing membranes and is therefore less suitable, given that an occlusive patch was desired as explained earlier.

3.2.2. Tensile properties of backing membranes

Considerable differences were found in the stress-strain profiles, Young's modulus and yield stress of the backing membranes (Fig. 5, Table 5). CoTran 9701, had the lowest yield stress of 5 MPa, with the stress levelling off beyond this point and thus was the easiest membrane to deform, in contrast to Scotchpak 9723, 9733 and 9757, which showed plastic-strain hardening, i.e. an increase in the stress with increasing strain beyond the initial yield stress.

3.2.3. Behaviour of the backing membranes in peel tests

Peel tests were performed on backing membrane-PSA combinations adhered to the model HDPE nail substrate. During removal of a patch from a nail plate, a clean interfacial failure at the patch-substrate interface is desired as shown in Fig. 6a and c. However, a clean interfacial failure was not always achieved. As may be seen from Fig. 6, in some instances, (a) the PSA fibrillated (Fig. 6b) sometimes leaving PSA residue on the backing and HDPE surfaces (Fig. 6d), (b) delamination occurred at both the backing membrane/PSA and the PSA/HDPE interfaces (Fig. 6e) or (c) full debonding did not occur due to the patch stretching during peeling (Fig. 6f).

The visual observations in Fig. 6 were reflected in the load-displacement curves obtained during the peel tests (Fig. 7a and b) and can be explained by the nature and tensile properties of the backing membranes. Patches containing the Scotchpak 9723 backing membrane showed a non-steady state peeling force profile, as they failed at both the backing-membrane/PSA and the PSA/substrate interfaces (see Fig. 6e). This is likely to be due to the fact that the Scotchpak 9723 backing membrane is composed of a polyethylene/polyester bilayer.
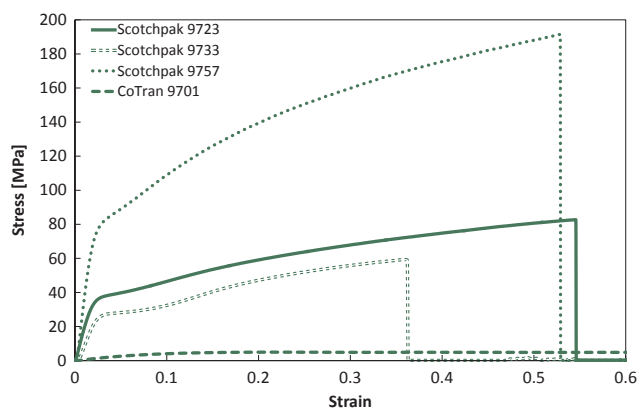
Table 4
The surface energies of the HDPE and Vitro-Nail model nail plates and of the selected PSAs. NA: not applicable. NT: not tested; amorolfine HCl-loaded Duro-Tak 2852 was not tested.

	Surface energies [mJ/m^2]			Work of adhesion, ψ_a [mJ/m^2]	
	γ_s^d	γ_s^p	γ_s	HDPE	Vitro-Nail
HDPE	37	1	38	NA	NA
Vitro-Nail	44	6	50	NA	NA
Human nail*			*34.1 $\pm$ 5.5		
Duro-Tak 2852	29	0.8	29.8	68	76
2852 + ciclopirox olamine	28	1.1	29.1	67	76
2852 + amorolfine HCl	NT	NT	NT	NT	NT
Duro-Tak 202A	34	0.1	34.1	72	79
202A + ciclopirox olamine	31	0.0	31.0	69	75
202A + amorolfine HCl	30	0.2	30.2	68	75

* Value of surface energy of human nail measured in vivo from [26].

Table 5
Properties of backing membranes tested. Means and SDs are shown.

Backing membrane	Material (colour) from Technical Data Sheets	Thickness (μm) N = 4–5	Vapour transport (mg/cm^2/day) N = 4–5	Young's Modulus (GPa) N = 7–9	Yield Stress (MPa) N = 7–9
Scotchpak 9757	Polyester film (transparent)	14.0 $\pm$ 1.6	2.9 $\pm$ 0.06	4.31 $\pm$ 0.16	70 $\pm$ 4.3
Scotchpak 9733	Laminate of polyester and an ethylene vinyl acetate copolymer layer (translucent)	48.5 $\pm$ 1.9	2.3 $\pm$ 0.55	1.38 $\pm$ 0.08	24 $\pm$ 1.4
Scotchpak 9723	Laminate of pigmented polyethylene and polyester (tan)	38.8 $\pm$ 1.0	2.2 $\pm$ 0.46	1.95 $\pm$ 0.05	37 $\pm$ 3.1
CoTran 9701	Polyurethane film (translucent)	50.3 $\pm$ 0.5	19.4 $\pm$ 0.29	0.054 $\pm$ 0.005	5 $\pm$ 0.4

Fig. 5. Tensile stress-strain curves of Scotchpak 9723, 9733 and 9757 and CoTran 9701 backing-membranes at test speeds of 100 mm/min.

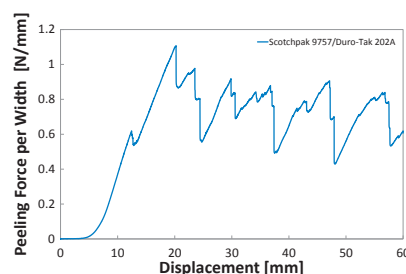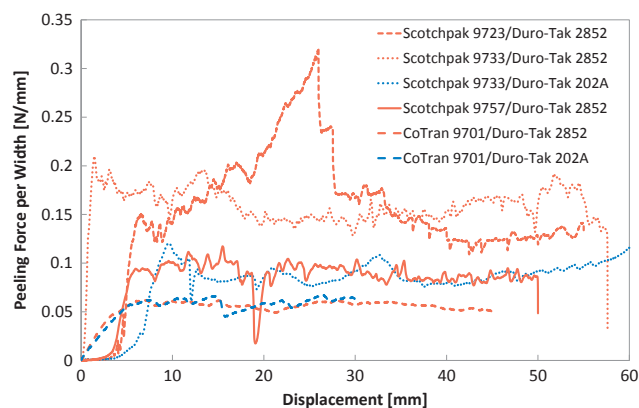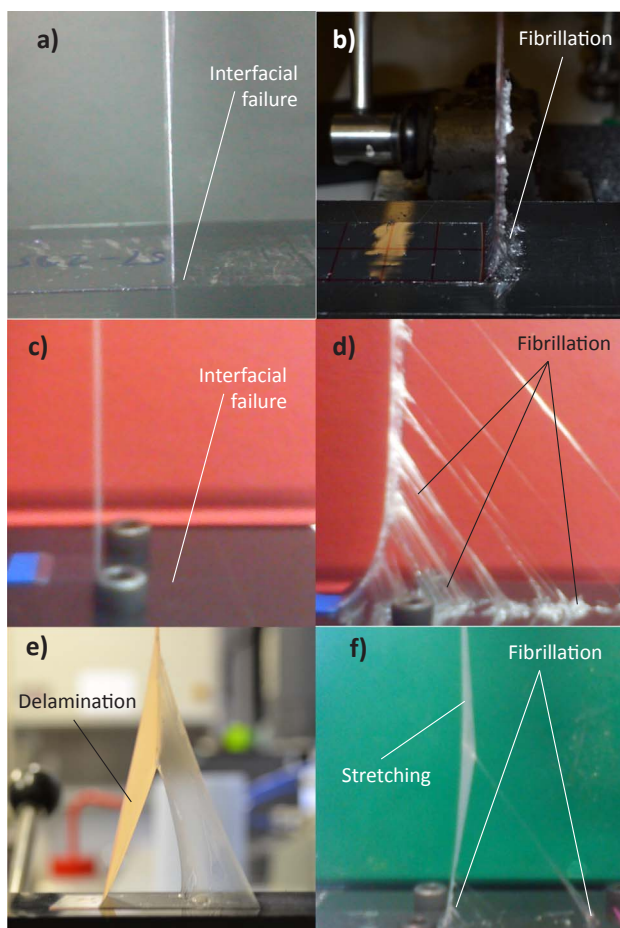**Fig. 6.** Various peeling behaviours of backing membrane-PSA combinations adhered to the HDPE substrate: (a) Scotchpak 9757/Duro-Tak 2852; (b) Scotchpak 9757/Duro-Tak 202A; (c) Scotchpak 9733/Duro-Tak 2852; (d) Scotchpak 9733/Duro-Tak 202A; (e) Scotchpak 9723/Duro-Tak 2852; (f) CoTran 9701/Duro-Tak 202A. The same failure mechanism, as shown in (f) was found for the CoTran 9701/Duro-Tak 2852 combination.

Fig. 7. a and b. Typical peel force-displacement curve, for different backing membrane-PSA combinations.

During the peel test, the PSA was sandwiched between two materials (i.e. the polyethylene surface of the backing membrane and the HDPE substrate) which possessed relatively similar surface energies. Thus, similar intrinsic adhesion existed at both the backing-membrane/PSA and at the PSA/HDPE interfaces which had led to the patch debonding at both interfaces during peeling. Meanwhile, patches containing Co-Tran 9701 backing membrane showed very low peeling forces due to its relatively low modulus and yield stress (as shown in Table 5, which

resulted in incomplete patch-substrate debonding and patch stretching (see Fig. 6f). Considerably high peak peel forces with a stick-slip action due to the formation of fibrils at the peel front were obtained with the Scotchpak 9757/Duro-Tak 202A combination (Fig. 7b). In contrast the Scotchpak 9733/Duro-Tak 202A patch showed a relatively smooth continuous, force profile with less pronounced peaks and troughs due to the relatively large fibrils which were observed (see Fig. 6d). Patches containing the backing membranes Scotchpak 9757 or Scotchpak 9733 together with the Duro-Tak 2852 PSA showed relatively uniform steady-state peeling force profiles, reflecting the desirable clean interfacial failures seen in Fig. 6a and c.

3.2.4. Final selection of backing membranes from appearance, tensile and peel tests

From Sections 3.2.1– .2.3, CoTran 9701 and Scotchpak 9723 backing membranes were eliminated. CoTran 9701 backing membrane was eliminated due to its high moisture permeability and low modulus, which would result in non-occlusive patches that stretch and fail to debond fully during patch removal from a nail. Scotchpak 9723 backing membrane was eliminated due to patch debonding at both the backing-membrane/PSA and PSA/nail interfaces during patch peeling. These eliminations left Scotchpak 9733 and Scotchpak 9757 as potential backing membranes. As can be seen from Fig. 6a and c, the use of either backing membranes resulted in optimal patch peeling, when combined with Duro-Tak 2852 PSA, resulting in clean interfacial failure at the PSA/model nail interface. From these two choices, Scotchpak 9757 was favoured over Scotchpak 9733 due to a much lower peel force required for patch removal from a model nail plate and its higher Young's modulus and yield stress. These aspects mean that the Scotchpak 9757 backing membrane was (a) less likely to considerably deform, elastically or plastically, and hence the force required to remove the patch would not greatly increase during patch peeling off a nail in practice and (b) not likely to break during patch removal from a nail. Thus, Scotchpak 9757 was selected as the backing membrane for subsequent patch development.

3.3. Patch preparation and characterisation

Following the above selection of (a) the two PSAs (i.e. Duro-Tak 202A and Duro-Tak 2852), (b) the two drugs (i.e. ciclopirox olamine and amorolfine HCl), (c) the backing membrane (i.e. Scotchpak 9757) and (iv) the release liner (i.e. Scotchpak 9744), nail patches were prepared. Firstly, the PSAs (purchased as liquids where the PSA was dissolved in organic solvents with solid contents of 42.4 ± 0.4% w/w for Duro-Tak 202A PSA and 36.5 ± 0.3% w/w for Duro-Tak 2852 PSA) were diluted with DCM (i.e. a good solvent for both the drugs and the PSAs). Dilution was needed to reduce the viscosity, enable good spreading upon casting and the formation of uniform adhesive layers. Following PSA dilution, the drug was dissolved at the appropriate concentrations to reach saturation solubility in the PSA, the solution was cast onto the backing membrane, the organic solvent was evaporated off and the release liner was then applied to the PSA layer, to prepare nail patches. These nail patches, which were based upon our proposed systematic approach to the formulation of a simple drug-in-adhesive ungual patch, were characterised as described below.

3.3.1. Patch thickness, residual solvent, drug content and distribution

The patches were between 380 and 480 μm thick, with relatively good uniformity of thickness (Supplementary file, S2). Drug content was 3% w/w amorolfine HCl in Duro-Tak 202A, 5% w/w amorolfine HCl in Duro-Tak 2852, 5% w/w ciclopirox olamine in Duro-Tak 202A and 16% w/w ciclopirox olamine in Duro-Tak 2852. The drug concentration in the patch was selected to be slightly less than the drug levels at which drug crystals would start to appear (shown in Table 3), to ensure that all the loaded drug was fully dissolved in the PSA. The absence of drug crystals was confirmed using polarised light microscopy.

Except for the ciclopirox olamine in Duro-Tak 2852, only relatively low amounts of drug could generally be loaded in the PSA in the patches in the dissolved form due to the fairly low solvency of the PSAs for the drugs and the evaporation of most of the solvent during patch preparation, which resulted in low residual solvent levels of below 2% w/w in the patches (Supplementary file, S3). The drug was dispersed uniformly within the full thickness of the patches for 5% w/w amorolfine HCl in Duro-Tak 2852 patches, as shown by Raman spectra taken at eight depths (Supplementary file, S4). However, Raman depth profiling of the other three patches showed higher levels of the drugs in the top layer of the patches (Supplementary file, S4). This is probably due to some degree of drug movement during solvent evaporation, as the drugs travel to the top with the solvent and accumulate at the patch surface. Similarly, and for the same reason, XPS analysis of the patch surface and interior showed drug presence throughout the patch thickness, although drug levels in the patch was not totally uniform (Supplementary file, S5).

3.3.2. Drug stability in patches

Polarised light micrographs of patches stored under accelerated and long-term test conditions showed negligible crystallisation of ciclopirox olamine over the six months storage. Indeed, image analysis of the micrographs showed that drug crystals occupied areas of less than 1% (Supplementary file, S6). The limited drug recrystallization in the patches is in agreement with reports of a similar lack of crystallisation of ethinyl estradiol and levonorgestrel in Duro-Tak 2074 and Duro-Tak 202A acrylic PSAs [29] where the authors suggested that polymeric acrylic adhesives could have inhibitory effects on drug crystallisation due to their carboxyl/hydroxyl functional groups, which might act as hydrogen acceptors and donors, and thereby immobilise drug molecules and prevent crystallisation.

Periodic analysis of the drug content of the patches stored at 40 °C/ 75% RH showed a greater chemical stability of the amorolfine HCl compared to the ciclopirox olamine (Fig. 8). In both patches, amorolfine HCl levels remained at 100% of the initial concentration over
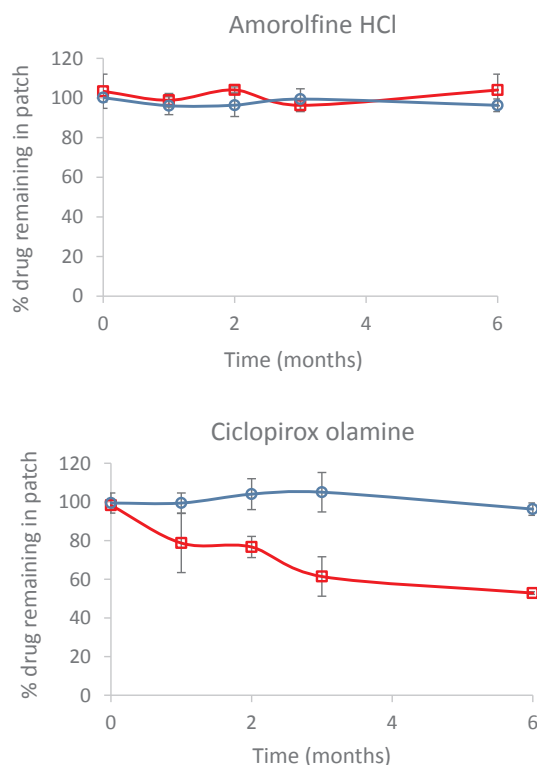
Fig. 8. The percentage of the drug remaining in the patch as a function of duration of storage (at 40 °C/75% RH). Patches contained Duro-Tak 202A (○) or Duro-Tak 2852 (□) PSAs. Means and SD (error bars) are shown. N = 3.

6 months. In contrast, while the ciclopirox olamine level remained the same in the Duro-Tak 202A based patch, its level in the Duro-Tak 2852 based patch decreased to about 50% of the initial drug load after six months. That is, in the latter case, the ciclopirox olamine was degrading with time. Furthermore, visual observations of the patches showed that the ciclopirox olamine loaded Duro-Tak 2852 based patches gradually became more yellow in colour with time (Supplementary file, S7). Greater degradation of ciclopirox olamine in Duro-Tak 2852 could be due to an inherent instability of the drug and/or be related to the nature of the adhesive. Duro-Tak 202A and Duro-Tak 2852 are both acrylic polymers, with differences in their functional groups (Table 1, and viscosity, *Tg* and Young's modulus (which are all higher for Duro-Tak 2852 as shown in Supplementary file, S8). It is possible that interaction between ciclopirox olamine and the carboxyl groups in the Duro-Tak 2852 PSA enhances drug degradation, which would be reflected in the greater ciclopirox olamine degradation reported in acidic media [30]. Ciclopirox olamine degradation in other formulations (based on Poloxamer 407) and the generation of a yellowish discolouration has also been reported [31], as has its degradation by sunlight and UV light [32]. It seems that ciclopirox olamine possesses an inherent instability, and the present results, and those from the literature, indicate that formulations using this drug would need to be formulated at higher pH and should be protected from light. Thus, for ciclopirox-olamine containing nail patches, light-excluding opaque backing membranes might be more appropriate than transparent ones.

3.3.3. Peel properties of patches

Patches containing Duro-Tak 2852 PSA and Scotchpak 9757 backing membrane, which demonstrated an acceptable peeling behaviour from the model HDPE nail plate (Figs. 6 and 7a) were selected to measure the peel force, which give an indication of how easy it would be for a patient to remove an ungual patch from their nail. Upon peeling from human cadaver nail or model nail (i.e. HPDE or Vitro-Nail) substrates, debonding occurred cleanly at the desired PSA/substrate
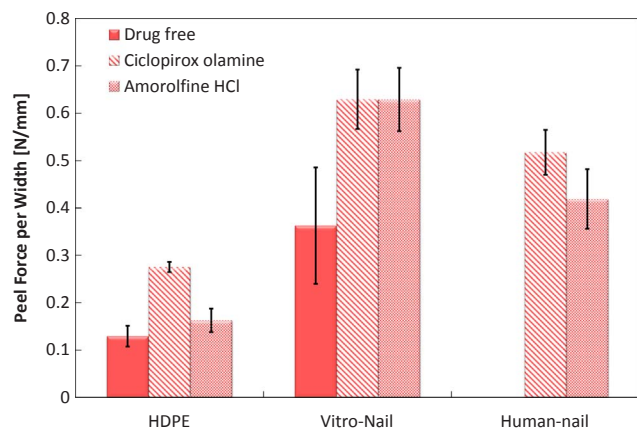
Fig. 9. The steady-state peel forces for drug-free and drug-loaded patches (composed of Duro-Tak 2852 PSA and Scotchpak 9757 backing-membrane) on different substrates. Means and SDs (error bars) are shown. N = 3–6.

interface for all three substrates, and the steady-state maximum peel forces are shown in Fig. 9. In general, the peel forces were lowest for the HDPE substrate, and highest for the Vitro-Nail substrate (two-way ANOVA, $p < 0.05$), reflecting the differences in their surface energies and the PSA-model nail thermodynamic works of adhesion (Table 4). However, the correlation is not perfect, with the peel forces for the HDPE substrate being lower than those for the human nail plate substrate ($p < 0.05$), despite their similar surface energies. It is possible that the higher peel forces obtained for the human nail were due to the higher surface roughness of the human nail, which would increase the surface area for adhesion and thereby increase the peel force. Drug loading in the patch increased the peel force ($p < 0.05$), with the two drugs having similar effects ($p > 0.05$). The lower peel force for the drug-free formulation can be correlated with the stiffer stress-strain response shown in Fig. 4, as stiffer adhesives often lead to lower peel forces [33]. Fig. 9 also shows that the patch/human nail peel forces are typically in between those for the patch/HDPE and patch/Vitro-Nail interfaces. Consequently, the HDPE and Vitro-Nail model substrates may be used as model nails for *in vitro* peel tests to give an indication of the forces required to remove ungual patches from human nails.

4. Conclusions

Our *aim* was to develop a new systematic approach to the formulation of drug-in-adhesive anti-onychomycotic nail patches, and in this paper, we demonstrate a possible pathway for such patch development. We started the proposed patch development methodology with the testing of each patch component individually, for example, testing the tensile properties of the possible PSAs. However, we have found that there are significant interactions between the patch components, for example PSA plasticisation by the drug and patch peeling behaviour dictated by PSA-backing membrane interactions. Thus, as we have demonstrated, it may be more appropriate to start the development methodology using combinations of patch components, and subsequently to assess the individual components of the most promising combinations, and then to select patch components and combinations for optimal formulation. The significant interactions among the patch components also mean that knowledge about the individual patch components may not always be transferable when a different drug is formulated.

From the work described in the present paper, the best patch formulation (one that is occlusive, can be peeled off the nail plate cleanly and where the drug remains stable upon patch storage) has been identified as one containing Scotchpak 9757 backing membrane, Duro-Tak 2852 PSA, the drug amorolfine HCl and Scotchpak 9744 release liner. The reported methodology paves the way for a systematic and

novel approach to the formulation of simple drug-in-adhesive ungual patches for the topical treatment of nail diseases.

Appendix A. Supplementary material

Supplementary data associated with this article can be found, in the online version, at https://doi.org/10.1016/j.ejpb.2018.02.032.

References

[1] P. Rich, R.K. Scher, An Atlas of Diseases of the Nail, The Parthenon Publishing Group, London, 2003.
[2] J.E. Arrese, G.E. Pierard, Treatment failures and relapses in onychomycosis: A stubborn clinical problem, Dermatology 207 (3) (2003) 255–260.
[3] D.P. Lubeck, D.L. Patrick, P. McNulty, S.K. Fifer, J. Birnbaum, Quality-of-life of persons with onychomycosis, Qual. Life Res. 2 (5) (1993) 341–348.
[4] S. Murdan, Nail disorders in older people, and aspects of their pharmaceutical treatment, Int. J. Pharm. 512 (2) (2016) 405–411.
[5] M.V. Saner, A.D. Kulkarni, C.V. Pardeshi, Insights into drug delivery across the nail plate barrier, J. Drug Target. 22 (9) (2014) 769–789.
[6] H.N. Shivakumar, A. Juluri, B.G. Desai, S.N. Murthy, Ungual and Transungual drug delivery, Drug Dev. Ind. Pharm. 38 (8) (2012) 901–911.
[7] T.S. Ahn, J.P. Lee, J. Kim, S.Y. Oh, M.K. Chun, H.K. Choi, Effect of pressure sensitive adhesive and vehicles on permeation of terbinafine across porcine hoof membrane, Arch. Pharmacal. Res. 36 (11) (2013) 1403–1409.
[8] Y. Myoung, H.K. Choi, Permeation of ciclopirox across porcine hoof membrane: effect of pressure sensitive adhesives and vehicles, Eur. J. Pharm. Sci. 20 (3) (2003) 319–325.
[9] R. Susilo, H.C. Korting, W. Greb, U.P. Strauss, Nail penetration of sertaconazole with a sertaconazole-containing nail patch formulation, Am. J. Clin. Dermatol. 7 (4) (2006) 259–262.
[10] R.F. Donnelly, P.A. McCarron, J.M. Lightowler, A.D. Woolfson, Bioadhesive patch-based delivery of 5-aminolevulinic acid to the nail for photodynamic therapy of onychomycosis, J. Control. Release 103 (2) (2005) 381–392.
[11] B. Amichai, B. Nitzan, R. Mosckovitz, A. Shemer, Iontophoretic delivery of terbinafine in onychomycosis: a preliminary study, Br. J. Dermatol. 162 (1) (2010) 46–50.
[12] M.B. Brown, G.P. Martin, S.A. Jones, F.K. Akomeah, Dermal and transdermal drug delivery systems: current and future prospects, Drug Delivery 13 (3) (2006) 175–187.
[13] H.S. Tan, W.R. Pfister, Pressure-sensitive adhesives for transdermal drug delivery systems, Pharm. Sci. Technol. Today 2 (2) (1999) 60–69.
[14] S. Venkatraman, R. Gale, Skin adhesives and skin adhesion 1. Transdermal drug delivery systems, Biomaterials 19 (13) (1998) 1119–1136.
[15] A.M. Wokovich, S. Prodduturi, W.H. Doub, A.S. Hussain, L.F. Buhse, Transdermal drug delivery system (TDDS) adhesion as a critical safety, efficacy and quality attribute, Eur. J. Pharm. Biopharm. 64 (1) (2006) 1–8.
[16] M. Ameen, J.T. Lear, V. Madan, M.F.M. Mustapa, M. Richardson, British Association of Dermatologists' guidelines for the management of onychomycosis 2014, Br. J. Dermatol. 171 (5) (2014) 937–958.
[17] H.B. Gunt, G.B. Kasting, Effect of hydration on the permeation of ketoconazole through human nail plate in vitro, Eur. J. Pharm. Sci. 32 (4–5) (2007) 254–260.
[18] W.R. Pfister, Transdermal and Topical Drug Delivery Systems, in: T.K. Ghosh, W.R. Pfister, S.I. Yum (Eds.), Buffalo Grove, Il, USA, Interpharm Press, 1997, pp. 33–112.
[19] C.M. Hansen, Solubility Parameters - An Introduction. Hansen Solubility Parameters A User's Handbook, C.M. Hansen (Ed.), Boca Raton, US, CRC Press, 2007.
[20] B. Hossin, K. Rizi, S. Murdan, Application of Hansen Solubility Parameters to predict drug-nail interactions, which can assist the design of nail medicines, Eur. J. Pharm. Biopharm.: Official J. Arbeitsgemeinschaft fur Pharmazeutische Verfahrenstechnik e.V 102 (2016) 32–40.
[21] S. Murdan, Transverse fingernail curvature in adults: a quantitative evaluation and the influence of gender, age, and hand size and dominance, Int. J. Cosmet. Sci. (2011).
[22] IMS, What are Vitro-Nails, 2015, (Retrieved 15 December 2016), 2016, from http://www.ims-usa.com/vitro-nails.
[23] S. Murdan, A. Bari, S. Ahmed, B. Hossin, L. Kerai, Nail lacquer films' surface energies and in vitro water-resistance and adhesionn do not predict their in vivo residence, Britixh J. Pharmacy 2 (1) (2017) 1–13.
[24] S. Murdan, L. Kerai, B. Hossin, To what extent do in vitro tests correctly predict the in vivo residence of nail lacquers on the nail plate? J. Drug Delivery Sci. Technol. 25 (2015) 23–28.

[25] A.J. Kinloch, G.K.A. Kodokian, J.F. Watts, The adhesion of thermoplastic fibre composites, Philos. Trans. Royal Soc. London Ser. A-Math. Phys. Eng. Sci. 338 (1649) (1992) 83–112.

[26] S. Murdan, C. Poojary, D.R. Patel, J. Fernandes, A. Haman, P.S. Saundh, Z. Sheikh, In vivo measurement of the surface energy of human fingernail plates, Int. J. Cosmet. Sci. 34 (3) (2012) 257–262.

[27] Y.G. Yao, X.S. Liu, Y.F. Zhu, Surface modification of high-density polyethylene by plasma treatment, J. Adhes. Sci. Technol. 7 (1) (1993) 63–75.

[28] 3M, M Scotchpak™ 972 Backing Tan Polyester Film Laminate, 2017. (Retrieved 20 January, 2017), from https://www.m.com/M/en_US/company-us/all-m-products/~/M-Scotchpak-972-Backing-Tan-Polyester-Film-Laminate?N=500285+29722892&rt=rud.

[29] M. Schulz, B. Fussnegger, R. Bodmeier, Drug release and adhesive properties of crospovidone-containing matrix patches based on polyisobutene and acrylic adhesives, Eur. J. Pharm. Sci. 41 (5) (2010) 675–684.

[30] B. Hossin, The rational design of an antifungal nail lacquer using the Hansen solubility parameter concept. PhD, University College London, 2015.

[31] A. Tauber, C.C. Muller-Goymann, In vitro model of infected stratum corneum for the efficacy evaluation of poloxamer 407-based formulations of ciclopirox olamine against Trichophyton rubrum as well as differential scanning calorimetry and stability studies, Int. J. Pharm. 494 (1) (2015) 304–311.

[32] B.H. Satani, J.V. Patel, R.B. Gami, C.N. Patel, Development and validation of a stability-indicating RP-HPLC method for estimation of Ciclopirox olamine in bulk drug and cream formulation, BioMedRx 1 (1) (2013) 102–108.

[33] I.K. Mohammed, M.N. Charalambides, A.J. Kinloch, Modelling the interfacial peeling of pressure-sensitive adhesives, J. Nonnewton. Fluid Mech. 222 (2015) 141–150.